

# A New Approach towards Precise Planar Feature Characterization Using Image Analysis of FMI Image: Case Study of Gachsaran Oil Field Well No. 245, Southwest of Iran

Mosayeb Shafieezadeh\*<sup>1</sup>, Mansour Ziaee<sup>2</sup>, and Behzad Tokhmchi<sup>3</sup>

<sup>1</sup> Refuling Unit, NIOADC, Kermanshah Region, Iran

<sup>2</sup> Department of Petroleum Engineering, University of Shahroud, Shahroud, Iran

<sup>3</sup> Department of Petroleum Engineering, University of Shahroud, Shahroud, Iran

## ABSTRACT

Formation micro imager (FMI) can directly reflect changes of wall stratums and rock structures. Conventionally, FMI images mainly are analyzed with manual processing, which is extremely inefficient and incurs a heavy workload for experts. Iranian reservoirs are mainly carbonate reservoirs, in which the fractures have an important effect on permeability and petroleum production. In this paper, an automatic planar feature recognition system using image processing was proposed. The dip and azimuth of these features are detected using this algorithm to identify more precise permeability and the career of fluid in reservoirs. The proposed algorithm includes three main steps; first, pixels representing fractures are extracted from projected FMI image into location matrices  $x$  and  $y$  and the corresponding value matrix  $f(x, y)$ . Then, two vectors  $X$  and  $Y$  as the inputs of CFTOOL of MATLAB are produced by the combination of these three matrices. Finally, the optimum combination of sine function is fitted to the sine shape of pattern to identify the dip and azimuth of the planar feature. The system was tested with real interpretation FMI rock images. In the experiments, the average recognition error of the proposed system is about 0.9% for the azimuth detection and less than 3.5% for the dip detection and the correlations between the actual dip and azimuth with the determined cases are more than 90% and 97% respectively. Moreover, this automatic system can significantly reduce the complexity and difficulty in the planar feature detection analysis task for the oil and gas exploration.

**Keywords:** FMI, Stratums, Carbonate Reservoirs, Dip, Azimuth

## INTRODUCTION

As the oil and gas exploration becomes gradually complicated, the traditional well logging methods have many problems. With limited information, recognizing effective layers and estimating reserves

parameters become more and more difficult. In contrast, the formation micro imager (FMI) technology can provide rich information on fractured reservoirs, and most importantly it can be applied to identifying fractured reservoirs qualitatively and can help explain them quantitatively [1,2].

### \*Corresponding author

Mosayeb Shafieezadeh

Email: m.shafieezadeh@niopdc.ir

Tel: +98 9366406168

Fax: +98 83 4522 2022

### Article history

Received: May 24, 2014

Received in revised form: November 25, 2014

Accepted: December 31, 2014

Available online: July 26, 2015

The full-bore formation micro imager provides micro resistivity formation images in water-base mud. Micro resistivity changes are related to lithological and petrophysical variations in the rock, which are conveyed mainly by the high-resolution current component and are interpreted on the image in terms of rock texture, stratigraphic and structural features, and fractures. The physics of the FMI measurement makes it a geological and reservoir characterization tool which produces complete and reliable answer products. These real-time answers are used to characterize the structural dip and faults, identify and evaluate sedimentary features, measure the rock texture, and complement the information obtained from coring programs [3].

To our knowledge, we rarely find automatic structural feature recognition systems with FMI images in the literatures. Consequently, for promoting oil and gas exploration, it is of great significance to develop an efficient and intelligent recognition system using FMI images. For oil and gas reservoirs with FMI images, relative image analysis technologies are mainly for reservoir fracture detection and extraction. Ginkel et al. used the generalized Radon transform to detect fractures in FMI images, which mapped the original 2D image to a 3D orientation space. These methods focus on robust fracture detection and prediction, which are not directly related to rock classification. Furthermore, these fracture analysis techniques with some complicated algorithms are also based on a large number of image samples. Although, Yun et al. proposed an algorithm in 2009, which could be used for limited samples, this algorithm only was used for the classification of the limited type of volcanic rocks (Tuff, Lava, and Breccia).

The interpretation of the FMI log image can be used to estimate planar feature dip and strike. The projection of a planar feature on borehole images will be represented by a sine wave as seen in Figure 3. Because the borehole is very small in relation to stratigraphic and structural features,

when they intersect the borehole, they are nearly planar and assumed to be a planar feature; thus a sine function was used herein for fitting the best curve on the fracture pattern.

We analyze rock FMI images with very limited samples in a different way by using image processing. There are several key issues in such recognition systems for FMI images. Firstly, the training samples are limited in most cases due to sensitive company data source. Secondly, FMI images are usually of great noises. In practice, even with manual processing, it is very difficult to analyze and classify rock structures without enough expertise.

The rest of the paper is organized as follows: in section 2, basic information about FMI image is represented. Section 3 simply describes the recognition system and methodology. Conclusions and discussions are presented in section 4. Finally, the experimental results are shown in section 5.

## **EXPERIMENTAL PROCEDURES**

### **Placement**

The Gachsaran oil field is in the southwest of Iran containing several wells (Figure 1). The FMI image used in this paper is related to well 245 of this oil field.

### **FMI Image**

The formation micro imager (FMI) tool (Figure 2) provides a detailed view of stratigraphic, lithologic, and structural information along the wall of the well bore. The FMI tool provides an image with 80% coverage of the borehole wall in an 8 inch diameter borehole.

The spacing of the FMI tool electrodes offers a maximum resolution of 0.2 inches in the azimuthal and vertical directions and a detection limit of 50 microns (about 0.002 inches) in the horizontal direction.

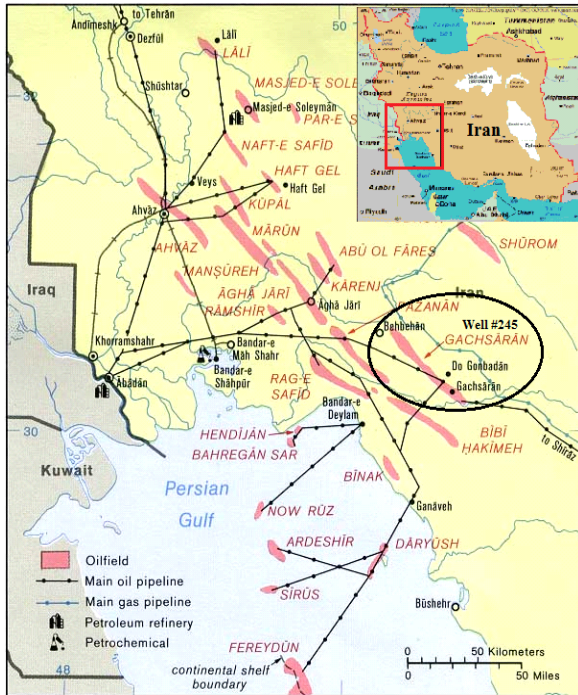


Figure 1: Gachsaran oil field location

The FMI tool uses an alternating current (AC) to produce a current map that minimizes the effects of a formation spontaneous potential (SP) and the direct current (DC) flow between the electrodes on the surface of the borehole (Schlumberger, 2002). The current is emitted through the lower electrodes and received by the upper electrodes after it has passed through the formation. The amount of current received is recorded and digitized [4].

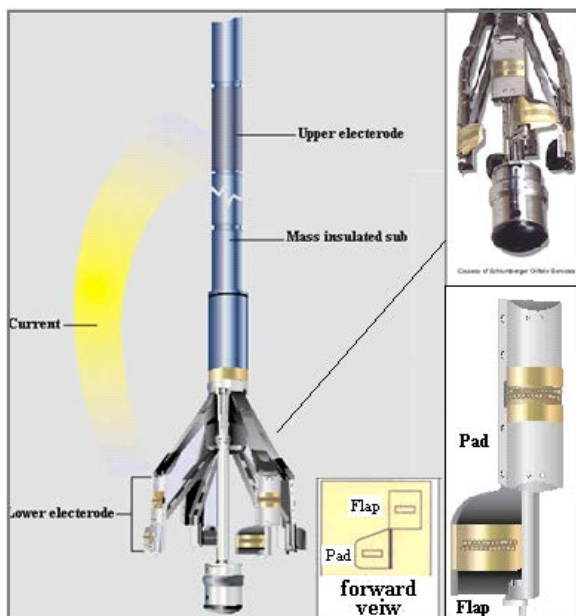


Figure 2: The FMI tool

Current values are recorded at points along the borehole wall. The variations of the measured current flow are portrayed as variations in the borehole color scheme to produce a resistivity image of the borehole (Figure 3). The current map color ranges from white to black with the lighter colors corresponding to relatively low conductivity zones and the darker colors denoting higher conductivity zones. The FMI tool also uses direct current induction to determine formation resistivity.

A typical FMI log header is shown in Figure 3. This header is divided into 7 vertical columns labeled in red. Column 1 provides depth and caliper readings. Column 2 displays a static current map image. The static current map is displayed in grey scale and represents the relative current at any positions in the borehole compared to the absolute highest and lowest current values obtained in the logging session. The static image is used to determine the major lithologic features surrounding the borehole. Column 3 shows the output of multiple induction logs. Generally, a shallow induction, medium induction, and a deep induction log are run with the FMI tool.

Column 4 is a depth and lithology indicator. The lithology indicator is obtained by combining the gamma ray, induction, and photoelectric effect of the rock being tested. This section provides a first approximation of formation lithology. The neutron and density porosity readings are plotted in Column 5. The log display also shows the amount of mudcake present in the borehole in Column 5. Column 6 displays the dynamic current map. Unlike the static current map, the dynamic current map recalculates the discrete current values every inch. This allows small scale features to stand out in the FMI dynamic current map image. Finally, column 7 illustrates the tadpole plots for the planar features interpreted in the FMI log. The circle of the tadpole plot is located at the depth and dip of the planar features. The dip scale is nonlinear and increases from 0 degrees (on left) to 90 degrees (on right).

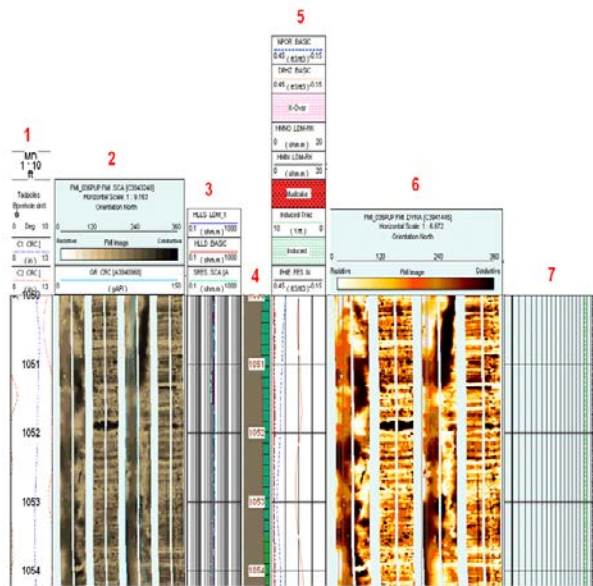


Figure 3: Typical FMI header information and log tracks; this log is from well 67-1-X-10 at Teapot Dome, Wyoming [4].

### Methodology

In FMI image, the trough of the sine wave, which represents the planar feature, indicates the azimuthal angle (dip trend angle) of this feature. Figure 4 portrays how the trough value of the sine wave corresponds to the azimuthal angle of the planar feature on the FMI image. The dip of the planar feature can be directly calculated from the amplitude of the sine wave and the diameter of the borehole. However, the difference between the maximum and minimum values of sine wave is used instead of the amplitude.

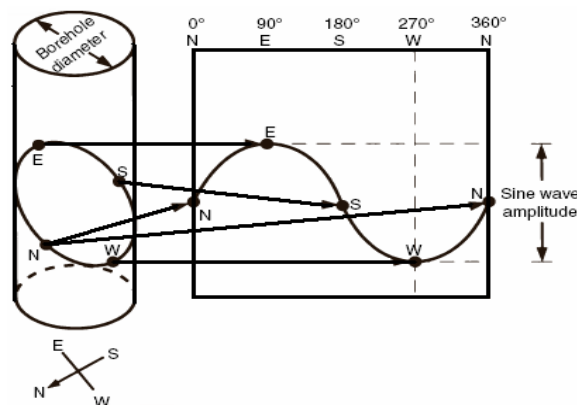


Figure 4: Displaying of directional information on the FMI log [4]

Our system extracts the proper dip and azimuth with FMI images automatically. This system includes three main steps. First, the pixels representing high conductivity locations are extracted from FMI image using a proper threshold into three matrices;  $x$ ,  $y$  and  $f(x,y)$ , which are the position and intensity of image pixels (Figure 5).

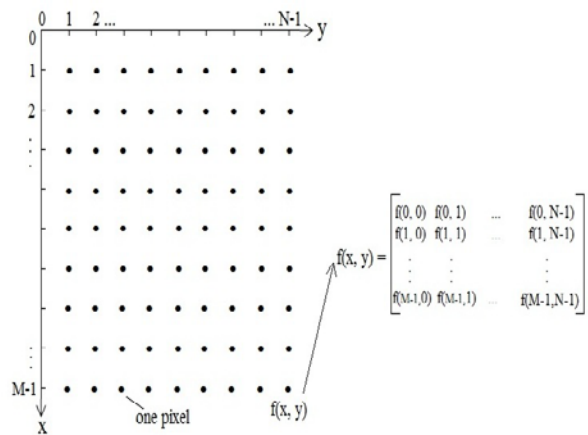


Figure 5: The position and intensity of image pixels

Then, the corresponding matrices are combined and two vectors are made: vectors  $X$  and  $Y$ . The size of these vectors must be equal.

Suppose that the image is composed by  $5 \times 9$  pixels;  $x$  and  $y$  matrices (vectors) are:

$$x = [0, 1, 2 \dots 4]; \text{ size } x = 5$$

$$y = [0, 1, 2 \dots 8]; \text{ size } y = 9$$

And the intensity function is given by:

$$f(x,y) = [ 30, 19, 28, 56, 16, 89, 15, 1, 0; 0, 108, 2, 50, 112, 89, 15, 180, 20; 0, 1, 200, 56, 6, 89, 150, 19, 200; 10, 15, 24, 150, 61, 189, 50, 81, 121; 90, 11, 42, 70, 116, 89, 15, 11, 2];$$

In this example, it is assumed that the intensity values above 100 are expectative values representing the position of planar features with low resistivity in FMI images.

In order to extract these pixels as two vectors  $X$  and  $Y$  (the inputs vectors of CFTOOL of MATLAB in which  $X_i$  versus  $Y_i$  is plotted), the following steps are conducted:

Use the following threshold:





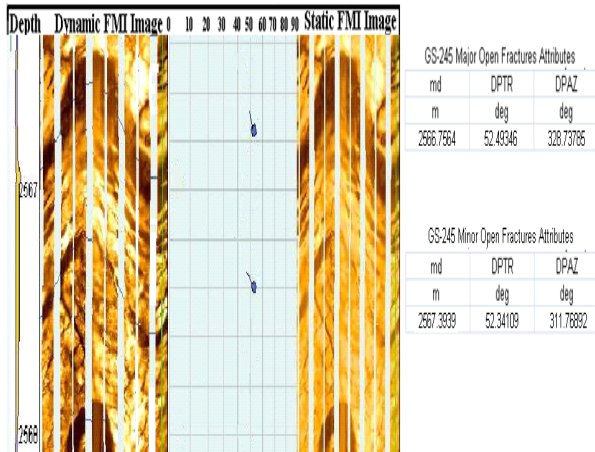


Figure 7: Fractures at depths of 2566 and 2567 m and their characterizations

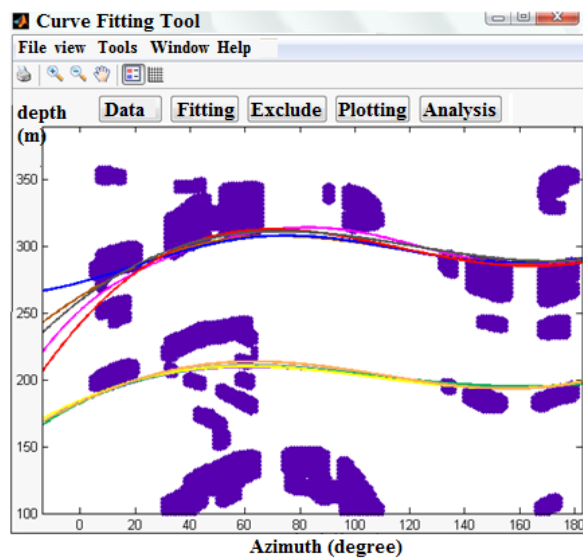


Figure 8: Fitted curve on planar feature pattern

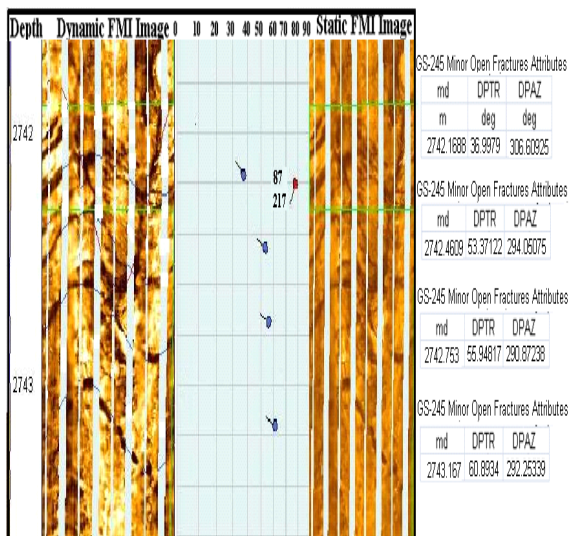


Figure 9: Conductive seam and planar features at depths of 2742 and 2743 m and their characterizations

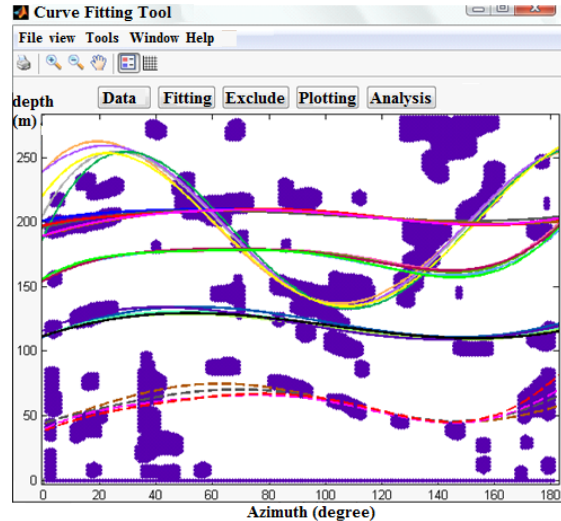


Figure 10: Fitted curve on planar feature pattern

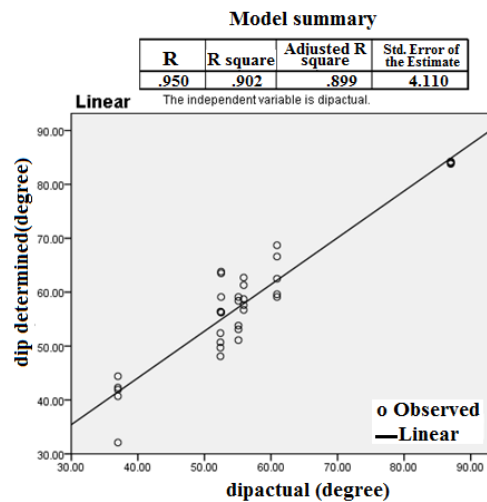


Figure 11: Amount of correlation between the algorithm results and the actual cases for dip detection using SPSS software

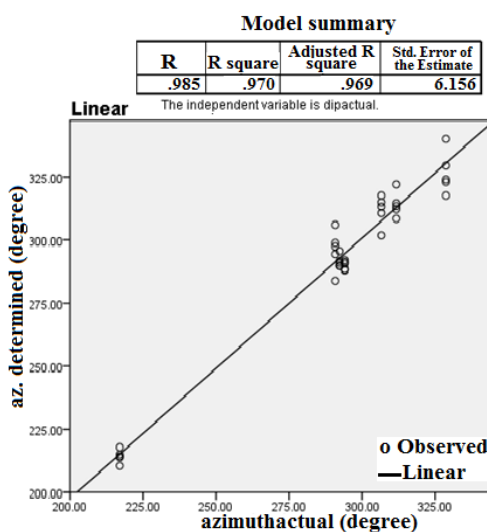


Figure 12: Amount of correlation between the algorithm results and the actual cases for azimuth detection using SPSS software

**Table 1: Extracted parameter ( $x$  and  $f(x)$ ) of critical points) from curves shown in Figures 7 and 10 for all the features**

Planar features	Depth	Parameter	Step 1		Step 2		Step 3		Step 4		Step 5	
			Min.	Max.	Min.	Max.	Min.	Max.	Min.	Max.	Min.	Max.
1	2742.2	$x$	156.6	78.5	158.8	62.8	157.5	76.3	150.9	58.2	155.3	71.4
		$f(x)$	197.4	209.9	198.2	209.8	198.8	209.8	200.7	208.7	197.9	209.4
2 (Conductive Seam)	2742.3	$x$	107.5	22.7	105.2	19.1	107.1	26.1	106.9	22	108.9	29.5
		$f(x)$	134.6	253.2	136.8	262.3	134.8	254.3	134.5	258.9	132.8	254.2
3	2742.5	$x$	144	66.3	145.3	78.3	146	70.4	144.2	66.2	145.6	76
		$f(x)$	162.3	179.3	162.6	178.4	157.1	178.4	158.6	179.4	160.9	178.4
4	2742.7	$x$	148.7	49.8	141.9	41.4	147.2	52.7	149.4	50.1	153	52
		$f(x)$	108.7	128.8	109.1	133.9	110.9	134.3	109.6	130.6	109.8	129.3
5	2743.2	$x$	144.8	47.9	144.9	78.4	147.8	62.6	145.8	69.3	145.4	75.4
		$f(x)$	43.3	76.1	45.1	66.9	45.3	74.8	45.7	70.3	44.6	65.9
6	2566.7	$x$	164.7	69.7	158.8	75.3	161.5	71.4	170	73.1	162	82.9
		$f(x)$	285.3	312.8	287.9	308.1	287.7	307.8	288.9	311.4	287.1	314.2
7	2567.4	$x$	154.2	60.4	156.7	63.3	157.3	62.9	156.1	61.8	161	61.4
		$f(x)$	193.7	210.2	193.4	213.7	193.8	211.3	193.8	209.7	195.2	210.2

**Table 2: General comparison between the determined dip with actual cases and the percentage of error**

Planar feature	Depth	Parameter	Step 1	Step 2	Step 3	Step 4	Step 5	Average	Actual	Percentage of error
1	2742.2	Dip	44.4	42.3	40.7	32.1	41.9	40.28	37	3.6
		Az.	313.2	317.6	315	301.8	310.6	311.64	306.6	1.4
(Conductive Seam)	2742.3	Dip	83.8	84.2	83.9	84.2	84	84.1	87	3.3
		Az.	215	210.4	214.2	213.8	217.8	214.3	217	0.8
3	2742.5	Dip	53.1	51.1	59.1	58.4	53.8	55.1	53.4	1.9
		Az.	288	290.6	292	288.4	291.2	290.1	294.1	1.1
4	2742.7	Dip	57.6	62.7	61.3	58.7	56.7	59.4	55.9	3.9
		Az.	297.4	283.8	294.4	298.8	306	296.1	290.8	1.5
5	2743.2	Dip	68.7	59.6	66.6	62.5	59.1	63.3	60.9	2.7
		Az.	289.6	289.8	295.6	291.6	290.8	291.5	292.3	0.2
6	2566.7	Dip	63.8	56.3	56.2	59.1	63.5	59.8	52.5	8.1
		Az.	329.4	317.6	323	340	324	326.8	328.7	0.5
7	2567.4	Dip	50.7	56.4	52.4	49.7	48.1	51.5	52.4	1
		Az.	308.4	313.4	314.6	312.2	322	314.2	311.7	0.7

**Table 3: Average percentage of error in dip and azimuth detection**

	Parameter	1	2	3	4	5	6	7	Average Error(%)
Error(%)	Dip	3.6	3.3	1.9	3.9	2.7	8.1	1	3.5
	Azimuth	1.4	0.8	1.1	1.5	0.2	0.5	0.7	0.88

## CONCLUSIONS

According to the result of the algorithm in dip and azimuth detection, this algorithm can determine these two important parameters of planar features (bedding, fault, or fracture) precisely. Since the average recognition error of our proposed system is about 0.9% for azimuth detection and less than 3.5% for dip detection, the correlations between actual dip and azimuth with the determined cases are more than 90% and 97% respectively. Moreover, this automatic system can significantly reduce the complexity and difficulty in the fracture detection analysis task for the oil and gas exploration. The algorithm can be improved to detect other parameters of fracture such as aperture.

## REFERENCES

- [1] Gonzalez R. C. and Woods R. E., *Digital Image Processing* (2<sup>nd</sup> ed.), Prentice-Hall, Inc. Upper Saddle River, New Jersey, **2002**, 69-164.
- [2] Gonzalez R. C., Woods R. E., and Eddins S. L., *Digital Image Processing using MATLAB*, Prentice-Hall, Inc. Upper Saddle River, **2004**, 1-104.
- [3] Schlumberger, "FMI Borehole Geology, Geomechanics and 3D Reservoir Modeling," Mark of Schlumberger, **2002**.
- [4] Schwartz B. C., "Fracture Pattern Characterization of the Tensleep Formation, Teapot Dome, Wyoming," Master Thesis, Department of Geology and Geography Morgantown, West Virginia, **2006**, 115-130.